

# ITERATIVE IMAGE RECONSTRUCTION FOR DUAL-ENERGY X-RAY CT USING REGULARIZED MATERIAL SINOGRAM ESTIMATES

Wonseok Huh and Jeffrey A. Fessler

Department of Electrical Engineering and Computer Science  
The University of Michigan  
1301 Beal Avenue, Ann Arbor, MI 48109-2122

## ABSTRACT

X-ray CT images have various applications, including CT-based attenuation correction (CTAC) for PET. Low-dose CT imaging is particularly desirable for CTAC. Dual-energy (DE) CT imaging methods may improve the accuracy of attenuation correction in PET. However, conventional DE CT approaches to sinogram material decomposition use logarithmic transforms that are sensitive to noise in low-dose scans. This paper describes a DE reconstruction method based on statistical models that avoids using a logarithm. We first estimate material sinograms directly from the raw DE data (without any logarithm), with mild regularization to control noise and avoid outliers. We then apply a penalized weighted least squares (PWLS) method to reconstruct images of the two material components. We also propose a joint edge-preserving regularizer that uses the prior knowledge that the two material images have many region edges located in the same positions. Preliminary simulation results suggest that this iterative method improves image quality compared to conventional approaches based on log data for low-dose DE CT scans.

## I. DUAL-ENERGY RECONSTRUCTION

### I-A. Measurement model

Let  $\mu(\vec{x}, \mathcal{E})$  denote the object's linear attenuation coefficient (LAC) which depends on the spatial position  $\vec{x}$  and the photon energy  $\mathcal{E}$ . For  $m = 1, \dots, M_0$ ,  $i = 1, \dots, N_d$ , the CT measurement data  $y_{mi}$  recorded by the  $i$ th ray for the  $m$ th incident spectrum has the following ensemble mean:

$$\bar{y}_{mi} \triangleq \int I_{mi}(\mathcal{E}) \exp\left(-\int_{\mathcal{L}_i} \mu(\vec{x}, \mathcal{E}) d\ell\right) d\mathcal{E} + r_{mi}. \quad (1)$$

where  $\int_{\mathcal{L}_i} \cdot d\ell$  denotes the line integral along the  $i$ th ray,  $I_{mi}(\mathcal{E})$  denotes the product of the  $m$ th incident source spectrum and the detector gain for the  $i$ th ray, and  $r_{mi}$  denotes additive background contributions such as room background, dark current, and scatter. We assume that  $I_{mi}(\mathcal{E})$  and  $r_{mi}$  are known nonnegative constants by [1]–[3].

This work was supported in part by NIH/NCI grant 1R01CA115870.

The measurements are finite, but  $\mu(\vec{x}, \mathcal{E})$  is a continuous function of  $\vec{x}$  and  $\mathcal{E}$ . Thus, for reconstruction we parameterize  $\mu(\vec{x}, \mathcal{E})$  using basis material decomposition [4] as follows:

$$\mu(\vec{x}, \mathcal{E}) = \sum_{l=1}^{L_0} \sum_{j=1}^{N_p} \beta_l(\mathcal{E}) b_j(\vec{x}) \rho_{lj}, \quad (2)$$

where  $\beta_l(\mathcal{E})$  denotes the energy-dependent mass-attenuation coefficient (MAC) of the  $l$ th material type; we use tabulated MAC values for water and bone [5].  $\{b_j(\vec{x})\}$  denotes unitless spatial basis functions such as square pixels, and  $\rho_{lj}$  are unknown density of  $l$ th material type at spatial location  $j$ . In DE CT, we usually choose  $M_0 = 2$ ,  $L_0 = 2$ .

Substituting (2) into (1) yields the following simplified model for the ensemble means of the measurements :

$$\bar{y}_{mi}(\mathbf{s}) = I_{mi} e^{-f_{mi}(\mathbf{s})} + r_{mi} \quad (3)$$

$$f_{mi}(\mathbf{s}) \triangleq -\log v_{mi}(\mathbf{s}) \quad (4)$$

$$v_{mi}(\mathbf{s}) \triangleq \int p_{mi}(\mathcal{E}) e^{-\beta(\mathcal{E}) \cdot \mathbf{s}_i} d\mathcal{E},$$

for  $m = 1, \dots, M_0$ ,  $l = 1, \dots, L_0$ , and  $I_{mi} = \int I_{mi}(\mathcal{E}) d\mathcal{E}$  denotes the total intensity for the  $m$ th incident spectrum and the  $i$ th ray, and we define the sinogram vector  $\mathbf{s}_i$  as follows:

$$p_{mi}(\mathcal{E}) \triangleq I_{mi}(\mathcal{E})/I_{mi}, \quad \beta(\mathcal{E}) \triangleq (\beta_1(\mathcal{E}), \dots, \beta_{L_0}(\mathcal{E})), \\ s_{il}(\rho) \triangleq [A\rho]_i, \quad \mathbf{s}_i(\rho) \triangleq (\mathbf{s}_{i1}(\rho), \dots, \mathbf{s}_{iL_0}(\rho)),$$

where  $A$  denotes the  $N_d \times N_p$  system matrix having elements

$$a_{ij} \triangleq \int_{\mathcal{L}_i} b_j(\vec{x}) d\ell.$$

In DE CT, the goal is to reconstruct the object density maps  $\rho_{lj}$  from the sinogram data.

### I-B. Conventional approach

Due to the nonlinear model (1), it is challenging to estimate the object  $\rho$  directly. Therefore, conventional methods first estimate the nonlinear function  $f_{mi}$  by inverting (3):

$$\hat{f}_{mi} \triangleq -\log\left(\text{smooth}\left\{\frac{Y_{mi} - r_{mi}}{I_{mi}}\right\}\right), \quad (5)$$

where radial smoothing is often included to reduce noise [6]. Then one applies conventional DE decomposition [4], followed by FBP reconstruction. This approach is fast but suboptimal especially for low-dose X-ray CT.

Recently, several iterative methods were presented, such as single energy CT [7], and statistical sinogram restoration for DECT [8], and PWLS DE CT reconstruction from  $\hat{f}$  [9]. At each iteration, the DE methods estimate the material images or material sinograms based on  $\hat{f}$ . However, accuracy of  $\hat{f}$  limits these methods;  $\hat{f}$  in (5) uses the logarithm that is sensitive to noise especially when  $y_{mi} - r_{mi}$  is small. Fig. 1 summarizes several possible methods for DE CT reconstruction.

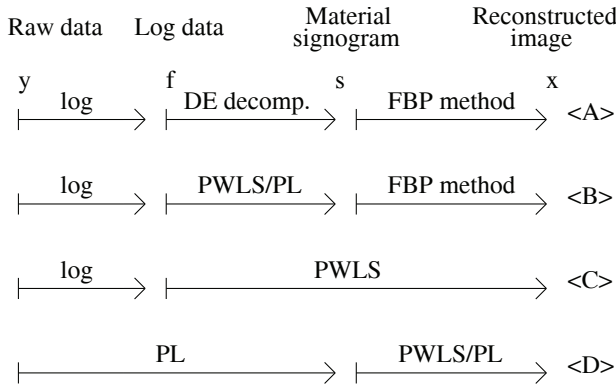


**Fig. 1.** Four different DE CT reconstruct algorithms. <A> conventional method [4], <B> statistical sinogram restoration [8], <C> PWLS DE CT reconstruction from  $\hat{f}$  [9], <D> proposed method.

### I-C. Proposed approach

This paper proposes a regularized iterative algorithm to estimate the material density map. This algorithm consists of two steps: (i) estimating material sinograms  $\hat{s}$  directly from the raw sinograms, and (ii) reconstructing the material density  $\rho$  from the estimated material sinogram. We use suitable regularization for both steps.

Instead of estimating  $f$  by using log function, we propose to estimate material sinogram,  $s$ , from X-ray CT measurement data,  $y$ , directly. By including a sinogram-domain roughness penalty  $R$  in the cost function, we can also control noise and handle cases where  $y_{mi} - r_{mi}$  is negative. Our cost function is defined as:

$$\hat{s} = \arg \min_s \Psi_1(s), \quad (6)$$

$$\begin{aligned} \Psi_1(s) &\triangleq L(s) + \beta_1 R(s) \\ &= \sum_m \sum_i \frac{w_{mi}}{2} |y_{mi} - \bar{y}_{mi}(s)|^2 + \beta_1 R(s), \end{aligned} \quad (7)$$

where  $s \triangleq (s_1, \dots, s_{N_d})$ ,  $s_i \triangleq (s_{i1}, \dots, s_{iL_0})$ , and

$$w_{mi} \triangleq \frac{1}{\text{Var}(y_{mi})}. \quad (8)$$

We minimize (7) using a CG algorithm with a monotone line search [10].

After estimating the material sinogram  $\hat{s}$ , we use it as the data fitting term to estimate the object  $\rho$  by minimizing the following cost function:

$$\hat{\rho} = \arg \min_{\rho} \Psi_2(\rho), \quad (9)$$

$$\begin{aligned} \Psi_2(\rho) &\triangleq L(\rho) + \beta_2 R(\rho) \\ &= \sum_l \sum_i \frac{\tilde{w}_{il}}{2} |\hat{s}_{il} - s_{il}(\rho)|^2 + \beta_2 R(\rho), \end{aligned} \quad (10)$$

where by error propagation (assuming  $\beta_1$  small):

$$[\text{diag}\{\tilde{w}_{i1}, \dots, \tilde{w}_{iL_0}\}]^{-1} \quad (11)$$

$$\approx \text{Cov}\{\hat{s}_i\} \approx (\nabla y_i)^{-1} \text{Cov}\{\hat{y}_i\} [(\nabla y_i)^{-1}]' \quad (12)$$

$$\approx (\nabla y_i)^{-1} \text{diag}\{Y_{mi}\} [(\nabla y_i)^{-1}]'. \quad (13)$$

The regularizer in (10) is given by:

$$R(\rho) = \sum_{l=1}^{L_0} \sum_{j=1}^{N_p} \sum_{k \in \mathcal{N}_j} \psi(\rho_{lj} - \rho_{lk}), \quad (14)$$

where  $\psi$  is a potential function and  $\mathcal{N}_j$  is a neighborhood of pixel  $j$  and the modified regularizer in [11] to provide uniform spatial resolution. For  $\psi$  we used a modified hyperbola discussed below. We define (7) similarly.

We minimized the cost function (10) using an ordered subsets method [12]. We initialized the iterations using the estimated image by the conventional algorithm in [9] and by using a suitable stopping criteria; the number of iterations did not exceed 200.

### I-D. Joint edge preserving regularizer

Previously we used a hyperbolic potential function  $\psi$  to preserve edges. However, this penalty function ignores the fact that water and bone material images share many common edges. To improve the accuracy of the algorithm, we should consider both materials' edge positions jointly when we estimate the object. Adapting [13], we investigated the following potential function:

$$\psi(\Delta\rho_1, \Delta\rho_2) = \sqrt{1 + \left(\frac{\Delta\rho_1}{\delta}\right)^2 + \left(\frac{\Delta\rho_2}{\eta}\right)^2} - 1 \quad (15)$$

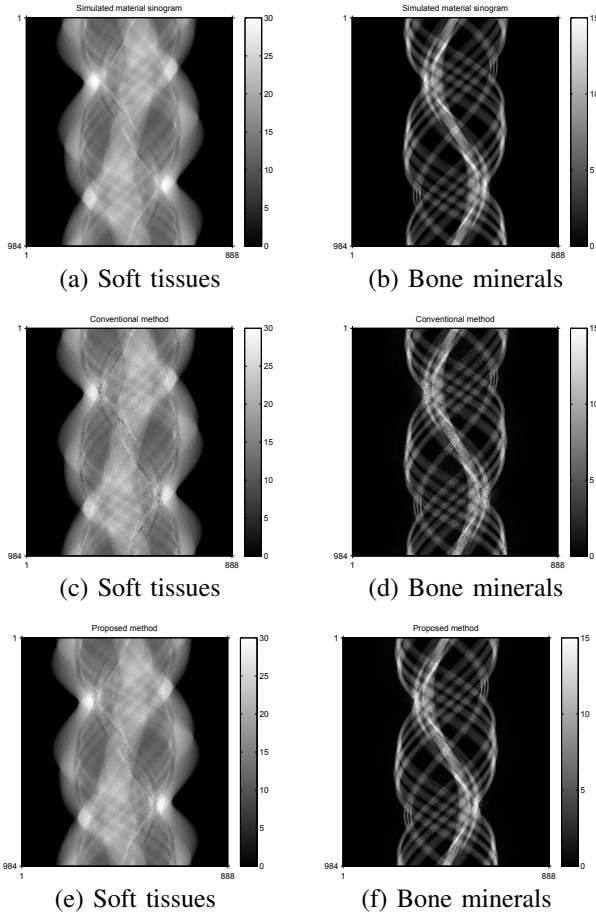
and the following roughness penalty function:

$$\begin{aligned} R(\rho_1, \rho_2) &= \sum_j \sum_{i \in \mathcal{N}_j} \psi(\rho_{1j} - \rho_{1i}, \rho_{2j} - \rho_{2i}) \\ &= \sum_j \sum_{i \in \mathcal{N}_j} \sqrt{1 + \left(\frac{\rho_{1j} - \rho_{1i}}{\delta}\right)^2 + \left(\frac{\rho_{2j} - \rho_{2i}}{\eta}\right)^2}, \end{aligned}$$

where  $\mathcal{N}_j$  denotes the neighborhood of pixel  $j$ . We need set the values of  $\delta$  and  $\eta$  differently due to the differences of the two material images; roughly we want  $\delta^2 \propto \text{Var}(\rho)$  to preserve edges while suppressing noise.

## II. RESULTS

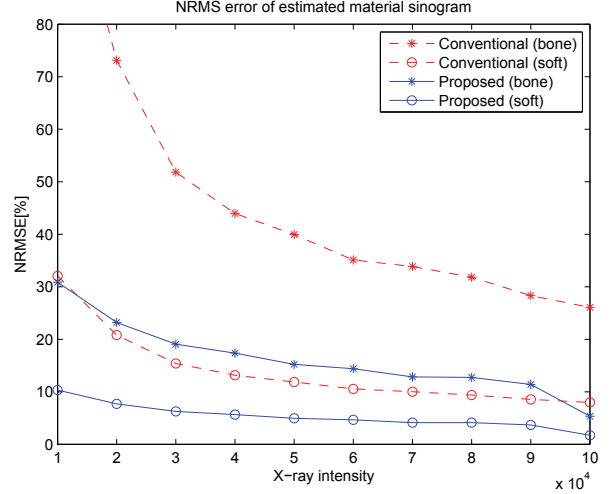
We simulated DE CT scans to evaluate the proposed methods feasibility for image reconstruction. The reconstructed images were  $128 \times 128$  with  $0.1 \times 0.1 \text{ cm}^2$  pixel size. The fan-beam projection space was 888 radial samples  $\times$  984 angular views over  $360^\circ$  degrees, with source voltages 80kVp and 140kVp. We applied the conventional dual-energy FBP reconstruction method, DE CT reconstruction algorithm in [9], and proposed method. We investigated 10 different X-ray source intensities, from  $1 \times 10^4$  to  $1 \times 10^5$  photons per ray.



**Fig. 2.** First row: simulated sinogram of two components. Second row: previous method <B> sinogram images with  $I_0 = 2 \cdot 10^4$ . Third row: proposed method <D> sinogram images with  $I_0 = 2 \cdot 10^4$ .

Fig. 2 illustrates estimated material sinograms based on the conventional logarithm approach, and the proposed method. The proposed method has reduced noise and outliers.

Fig. 3 shows that the proposed method reduces significantly the NRMSE of the material sinograms compared to the conventional sinogram estimation based on log function.



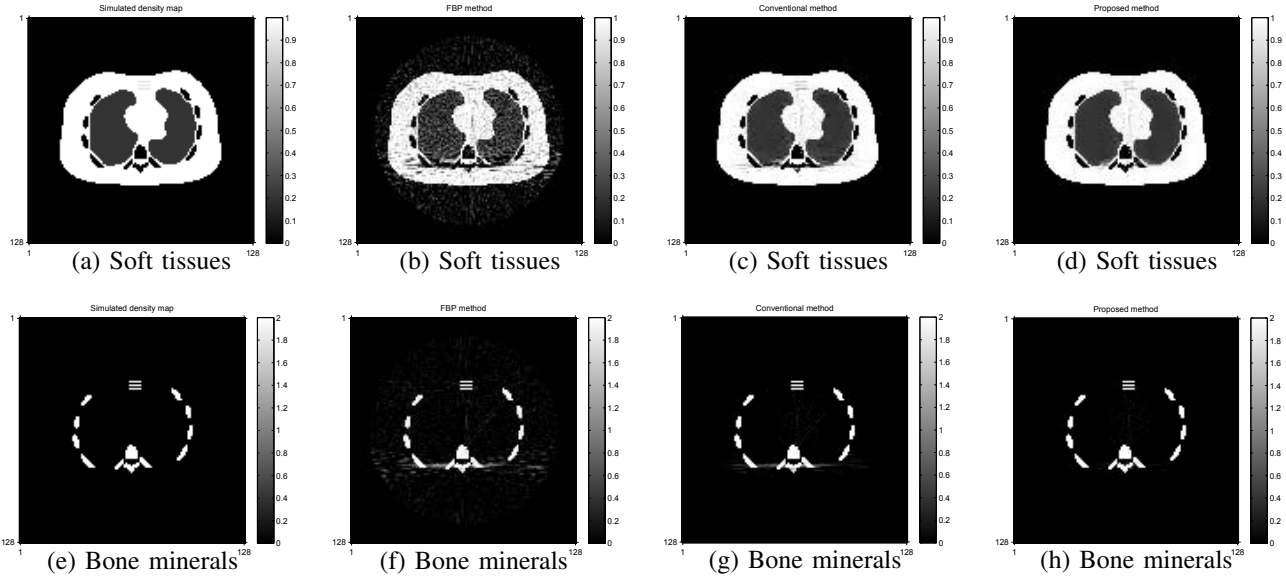
**Fig. 3.** NRMSE of reconstructed material sinograms: previous method <B>, and the proposed method <D>, versus  $I_0$  (number of incident X-ray photons per ray).

Fig. 4 shows the density maps of the material components: soft tissues and bone mineral and the estimated object of the three methods with  $I_0 = I_{mi} = 2 \cdot 10^4$ . Fig. 4(a)-(b) shows the simulated two component images. Fig. 4(c)-(d) shows FBP method images, whereas Fig. 4(e)-(f) shows the conventional iterative method images. The conventional iterative method succeeded in reducing streak artifacts compared to the FBP images. However, the conventional method image contains many outlier voxels whose magnitudes are larger than  $5 \text{ g/cm}^3$  even though the bone density is at most 2 here. In contrast, the proposed method, in Fig. 4(g)-(h), has successfully reduced streaks and yields lower noise than other two methods. Plus, its voxels have more reasonable density values for all spatial locations than the conventional approaches.

Fig. 5 shows the RMSE plot of the reconstructed object images with different incident intensities,  $I_0$ . We observed that the proposed method significantly reduces the NRMSE of soft tissue and bone minerals compared to the competing method.

## III. CONCLUSION

We presented a new iterative approach for DE CT reconstruction. Unlike other DE CT algorithms, the proposed method first estimates material component sinograms directly from X-ray DE CT sinograms without using a logarithm. Preliminary simulation results show that the proposed method estimates material sinograms more precisely than the conventional logarithm method. The improved sinograms yield images with lower RMS error than the conventional approach in Fig. 5. Our next step is to evaluate the method with a third material and compare to the method <C>.



**Fig. 4.** First column: Two component simulated densities. Second column: FBP method  $\langle A \rangle$  with  $I_0 = 2 \cdot 10^4$ . Third column: previous method  $\langle B \rangle$  with  $I_0 = 2 \cdot 10^4$ . Fourth column: proposed method  $\langle D \rangle$  with interpolated DE data.

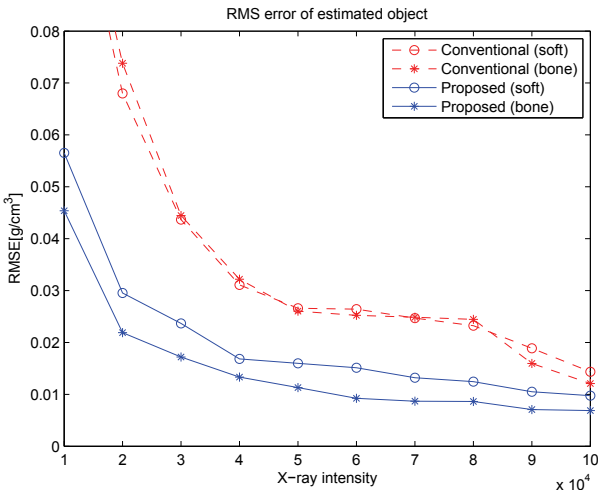


**Fig. 5.** RMSE of reconstructed object images: previous method  $\langle B \rangle$ , and the proposed method  $\langle D \rangle$ , versus  $I_0$  (number of incident X-ray photons per ray).

#### IV. REFERENCES

- [1] D. L. Snyder, C. W. Helstrom, A. D. Lanterman, M. Faisal, and R. L. White, "Compensation for readout noise in CCD images," *J. Opt. Soc. Am. A*, vol. 12, no. 2, pp. 272–83, Feb. 1995.
- [2] C. Ruth and P. M. Joseph, "Estimation of a photon energy spectrum for a computed tomography scanner," *Med. Phys.*, vol. 24, no. 5, pp. 695–702, May 1997.
- [3] A. P. Colijn and F. J. Beekman, "Accelerated simulation of cone beam X-ray scatter projections," *IEEE Trans. Med. Imag.*, vol. 23, no. 5, pp. 584–90, May 2004.
- [4] R. E. Alvarez and A. Macovski, "Energy-selective reconstructions in X-ray computed tomography," *Phys. Med. Biol.*, vol. 21, no. 5, pp. 733–44, Sept. 1976.
- [5] J. H. Hubbell and S. M. Seltzer, "Tables of X-ray mass attenuation coefficients and mass energy-absorption coefficients," 1995, National Institute of Standards and Technology <http://physics.nist.gov/PhysRefData/XrayMassCoef>.
- [6] J. Hsieh, "Adaptive streak artifact reduction in computed tomography resulting from excessive x-ray photon noise," *Med. Phys.*, vol. 25, no. 11, pp. 2139–47, Nov. 1998.
- [7] P. J. La Riviere, J. Bian, and P. A. Vargas, "Penalized-likelihood sinogram restoration for computed tomography," *IEEE Trans. Med. Imag.*, vol. 25, no. 8, pp. 1022–36, Aug. 2006.
- [8] J. Noh, J. A. Fessler, and P. E. Kinahan, "Statistical sinogram restoration in dual-energy CT for PET attenuation correction," *IEEE Trans. Med. Imag.*, vol. 28, no. 11, pp. 1688–702, Nov. 2009.
- [9] W. Huh, J. A. Fessler, A. M. Alessio, and P. E. Kinahan, "Fast kVp-switching dual energy CT for PET attenuation correction," in *Proc. IEEE Nuc. Sci. Symp. Med. Im. Conf.*, 2009, pp. 2510–5.
- [10] J. A. Fessler and S. D. Booth, "Conjugate-gradient preconditioning methods for shift-variant PET image reconstruction," *IEEE Trans. Im. Proc.*, vol. 8, no. 5, pp. 688–99, May 1999.
- [11] J. A. Fessler and W. L. Rogers, "Spatial resolution properties of penalized-likelihood image reconstruction methods: Space-invariant tomographs," *IEEE Trans. Im. Proc.*, vol. 5, no. 9, pp. 1346–58, Sept. 1996.
- [12] H. Erdoğan and J. A. Fessler, "Ordered subsets algorithms for transmission tomography," *Phys. Med. Biol.*, vol. 44, no. 11, pp. 2835–51, Nov. 1999.
- [13] X. He, J. A. Fessler, L. Cheng, and E. C. Frey, "Regularized image reconstruction algorithms for dual-isotope myocardial perfusion SPECT (MPS) imaging using a cross-tracer edge-preserving prior," *IEEE Trans. Med. Imag.*, 2010, To appear as TMI-2010-0116.